NTU Journal for Renewable Energy (2024) Vol. 7(1): 73-83
DOI: https://doi.org/10.56286/mry7bb56

ISSN: 2788-9912 (print); 2788-9920 (online)
NTU Journal for Renewable Energy
Available online at:
https://journals.ntu.edu.iq/index.php/NTU-JRE

Experimental Investigation of Solar Air Heater with Energy Storage Unit

Abdulrahman A. Mahmood[1], Ahmed M. Saleem[1]

[1]Engineering Technical College of Mosul, Northern Technical University, Cultural Group Street, Mosul, Iraq.

Article Information

Received: 17 July 2024
Received in Revised form: 1 August 2024
Accepted: 25 September 2024
Published: 10 October 2024

Corresponding Author:
Abdulrahman A. Mahmood

Email:
abdulrahman.ayad@ntu.edu.iq

Key words:
Solar System, Heat Storage, Cement Mortar Molds.

ABSTRACT

The present study investigates a single-pass solar air collector linked to a thermal energy storage unit. This system is designed to store energy using a cement mortar mold storage bed during daylight hours and reutilize it at night. A solar collector was used in this research, which was consecutively connected to the cement mortar mold bed. High-density cement mortar mold (570 kg) was used as a storage medium. The experiments were conducted on clear days for two random days at a constant airflow rate (0.0217 kg/s) for the climate of Mosul City, Iraq. The study assessed the parameters influencing the thermal performance of the solar air collector integrated with the cement mortar mold storage bed. Measurements of solar radiation intensity and air temperatures at various locations were recorded. The data indicated that the cement mortar mold storage bed achieved a temperature difference of approximately 10°C post-sunset, with this difference sustained for 4-5 hours. The cement mortar mold bed demonstrated the capability to retain heat for an extended post-sunset, releasing it during nighttime.

1. Introduction

The solar air collector (SAC) boasts a simple yet remarkably efficient design, cost-effectiveness, and effortless installation and upkeep. Its adaptability allows it many applications, including gathering heat [1]. Solar air heaters harness the sun's heat energy to heat the air, encompassing a crafted for heating homes, aiding agricultural drying processes, and ensuring convenient indoor temperatures, especially on colder days [2]. The efficiency of solar heating systems varies significantly based on geographical location and specific atmospheric conditions [3]. During periods when sunlight is scarce, implementing sustainable, eco-friendly solar heating solutions, like using solar air collectors for dispersing heated air, can face substantial obstacles. Effectively storing thermal energy becomes crucial to tackling intermittent and dispersed characteristics of solar power [4]. A suggestion has been made to employ a stone-centric energy storage mechanism to address the issue of energy consumption during periods of diminished sunlight, such as evenings or cloudy conditions [5]. Alomar O et al. [6] studied encompasses a practical inspection of adding porous material above the absorber flat platwith fins to improve solar air heaters' effectiveness. Outcomes emphasize that the effectiveness of an altered model was better than that of a traditional model by 7% for all air mass flow rate values. V. V. Tyagi et al. [7] investigated solar energy's time-dependent and intermittent nature. A widely advocated strategy entailed the conversion of solar Energy into thermal Energy. Singh et al. [8] studied packed-bed solar energy storage systems experimentally, focusing on materials used, packing material sizes, and system performance factors. Zho et al. [9] measured the appropriateness of sintered ore particles, aluminum oxide balls, and crushed rock as materials for sensible heat storage. Crushed rock was appropriate for heat storage at temperatures below 550 °C; sintered ore particles were identified as the superior material for storing heat at extremely high temperatures, up to 1000 °C. Hassan A. et al. [10] invented a transient thermodynamic model for a conical-shaped rock bed thermal energy storage (TES) system integrated with a hybrid V-groove double-pass solar air heater (SAH); they revealed that the maximum Energy recoverable during discharging was determined to be 33% of the stored energy, thereby satisfying the energy requirements for drying operations post-sunset. Heydari A. [11] investigated four types of apple, kiwi, banana slices, and quince julienne strips that had been dried using a cabin solar dryer equipped with a heating element as an auxiliary heat source. The results showed that thermal efficiency, drying process exergy, produced exergy, and specific moisture evaporation rate (SMER) of julienne quince strips are higher than those of other products. C. A. Komolafe et al. [12] carried out an investigative experiment that examined a locally made solar air heater and a thermal study with quadrilateral/.coarseness on the absorber layer. The thermal efficiency ranged from 14.0 to 56.5 percent. The temperatures recorded by experimental results ranged from 20 ºC to 112°C. Consequently, this resulted in the solar air heater demonstrating its ability to perform various tasks effectively, including desiccating various crops and heating water, all while controlling temperature.

In this study, an energy storage unit is added to the solar air heater to take advantage of the energy stored in this unit for the most extended possible period after sunset. The material used in the energy storage unit is

cement mortar molds that are made locally. This study is conducted in the city of Mosul, Iraq.

2. Experimental Setup

The experiment investigation set, apparatus, equipment, instruments, and tools were designed, rigged up, constituted, and installed at the Maan laboratories roof of the Technical Engineering College – Mosul. The system consists of a flat plate solar collector connected by a flex duct with a storage unit, such as the one depicted in Figure 1. The set for the system comprises the listed below units:

1. Solar collector.
2. Heat storage unit.
3. Cement mortar molds.
4. Temperature Data loggers.
5. Fan with speed controller.

A section view schematic diagram for all the system setup shows all the parts of the system; see Figure 2.

Figure 1. Real front photo of the rig.

2.1 Solar Collector

2.1.1 Design and Fabrication of Frame

The frame of the solar collector consists of three layers: two of them are wood, the outer layer is 0.75 cm, the inner layer is 1.5 cm, and between them is foam insulation with a 2 cm thickness. The dimensions of the collector from the outer frame are 158.5 cm × 108.5 cm, and the space between the plate and glass is 8 cm, as illustrated in Figure 3.

2.1.2 Plastic Air Ducts

Plastic air ducts 7.5 cm in diameter were installed and perforated to distribute and pass air throughout the solar collector and storage box, as shown in **Figure 4**.

2.1.3 Glass

The glass of the collector is a single type with a thickness of 4 mm; as illustrated in **Figure 5**.

2.2 Heat Storage Unit

2.2.1 Sides of the Storage Unit

The sides of the storage unit box consist of three layers: two layers of wood; the outer layer is 0.75 cm, the inner layer is 1.5 cm, and between them is foam insulation with 2 cm thickness. The dimensions of the storage unit box from the outer frame are (122 cm × 108 cm), and the height of the storage from the inside of the box is 100 cm.

2.2.2 Inside of the Storage Unit

The plastic ducts, perforated from the top and sides, are connected to the fan at the base of the unit; as shown Figure 6. The cement mortar molds are roofed next to and above the plastic ducts; as shown in Figure 7.

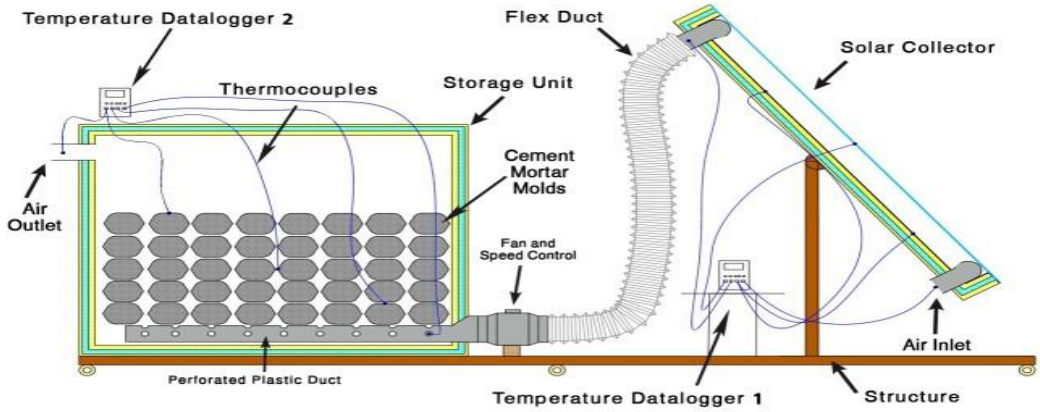

Figure 6. Section view schematic diagram of the rig

Figure 6. The frame of the solar collector.

Figure 6. Photo from the corner to show the glass.

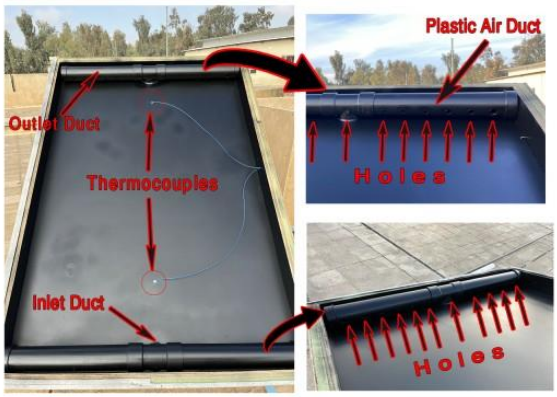

Figure 6. Photos show the inlet and outlet ducts and thermocouples of the SAC.

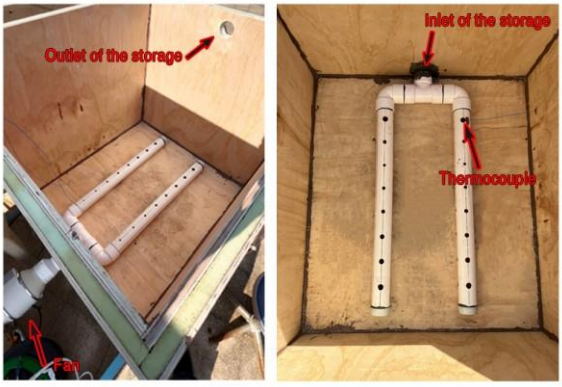

Figure 6. Plastic ducts inside the storage box.

Figure 7. Cement mortar molds, a photo from the top of the storage unit.

2.3 Cement Mortar molds

The storage component of the system is the cement mortar molds. The mixture of the cement mortar molds consisted of cement, sand, and water, which was poured into the molds, as illustrated in **Figure 8**. The weight of each mold is about 2.32 Kg. The total number of molds inside the storage is 245, and the total weight of the molds is 570 Kg. The volume of one mold is 0.0009 $m^{3,}$ and the density of the molds is 2577.778 Kg/m^3. Table 1 represents the physical properties of cement mortar molds.

Figure 8. Cement mortar molds.

Table 1 physical properties of the cement mortar molds and the air used in the experiment.

The density of the cement mortar molds (approximately)	2577.778 Kg/m^3
Specific heat of the Air	1.005 kJ/kg K
The mass flow rate of Air	0.0216475 kg/s
Total weight of the cement mortar molds (approximately)	570 Kg
Number of cement mortar molds (approximately)	245

2.4 Temperature Data loggers

Calibrated K-type thermocouples were used to measure temperatures in the inlet of the (SAC), outlet of (SAC), bottom of the absorption plate, top of the absorption plate, glass of the (SAC), inlet of the storage unit, outlet of the storage unit, bottom layer of the storage media, middle layer of the storage media and top layer of the storage media. The temperature thermocouples of previous components of the systems have been measured using a multi-channel thermometer with an accuracy of ±0.2°C. Handheld Multi-Channel Temperature Meter Data Logger type (Applent-AT4208) was used to record the temperatures from the thermocouples, such as the one depicted in Figure 9. The data logger has 8 channels to record the temperatures from the thermocouples. Two dataloggers have been used and 5 channels only for each datalogger connected with thermocouples are used as illustrated in **Figure 2**.

Figure 9. Applent-AT4208 Temperature Datalogger

2.5 Fan with speed controller

A fan of 40W is used to suck the hot air from the out of the collector and blow it to the storage unit, **Figure 10** shows the photo of the fan used.

Figure 10. Fan

3. Thermal Performance Evaluation

The cement mortar mold density was measured in the lab, and the average was 2577.778 Kg/m^3.
The void fraction (ε) can be determined using the equation below [13].

$$\varepsilon = \frac{V_1 - V_m}{V_1} \quad (1)$$

3.1 Efficiency of Energy Collection and Recovery ($\boldsymbol{\eta}$)

The solar Energy collected (Q_c) and Energy recovered (Q_{rc}) were calculated using the following equations [9]:

$$Q_c = \dot{m}\, C_p\, (T_{out} - T_{in}) \quad (2)$$

$$Q_{rc} = \dot{m}\, C_p\, (T_{out} - T_{in}) \quad (3)$$

The following formulae were used to calculate the collected and recovered energy efficiency. [14]:

$$\eta_c = \frac{\int_{t_1}^{t_2} Q_c\, dt}{\int_{t_1}^{t_2} IA\, dt} \text{ (Hourly)} \quad (4)$$

$$\eta_{rc} = \frac{\int_{t_1}^{t_2} Q_{rc}\, dt}{\int_{t_1}^{t_2} Q_c\, dt} \text{ (Hourly)} \quad (5)$$

During the calculation process, the heat dissipation to the atmosphere due to good insulation was not calculated.

3.2 Mass Flow Rate ($\dot{m}$).

This formula is used to calculate the mass flow rate of the air.

$$\dot{m}_{air} = \rho_{air}\, A\, V_{air} \quad (6)$$

3.3 Heat-transfer Coefficient Determination

An energy equation has been discovered empirically to estimate the effective thermal conductivity. In the literature, there are a number of heat-transfer correlations that may be used to determine the system's temperature distribution. The heat-transfer coefficient, which was developed by [15].

$$h = \frac{700}{6(1-\varepsilon)} G^{0.76} D_r^{\,0.24} \quad (7)$$

G the superficial mass flow rate, or air mass flux [16], is defined as:

$$G = \frac{\dot{m}}{A_{bed}} \quad (8)$$

Clark (1986) posits a relationship between the heat-transfer coefficient h and Reynold's number (10–10,000) for airflow through a bed of randomly packed spheres [16].

$$\frac{h\,D_r}{K} = 2 + 1.354Re_o^{0.5}Pr^{1/3} + 0.0326Re_oPr^{0.5} \quad (9)$$

Results and Discussion

An experimental study evaluated the heat performance results of a single-pass solar air heater with a cement mortar mold bed. The tests were applied for two months on clear days with a steady air flow rate (0.0217 kg/s). The two-day experimental tests were randomly selected for Mosul City, Iraq, on February 26th and March 25th, 2024.

Error! Reference source not found. illustrate the relationships of solar irradiation, the air outlet temperature of the solar air collector, and ambient temperature over time. The temperature patterns at the inlet (ambient temperature) and the increase in the outlet temperature of the solar air collector demonstrate a correlated response to fluctuations in solar radiation intensity. Moreover, there is a noticeable difference between the outlet temperatures of the solar air collector and the ambient temperature observed across two different days, with values corresponding to the length of daytime.

On February 26th, 2024, **Error! Reference source not found.** shows that the outlet temperatures of the solar air collector attained their maximum values, an occurrence attributed to increased solar radiation intensity and a modest rise in ambient temperature. The solar radiation intensity reaches its maximum value at the zenith, which was 1070 W/m² between 11:30 A.M. and 12:30 P.M., consequently raising the collector's outlet temperature to 60.7°C.

Also **Error! Reference source not found.** gives the ambient temperature varied between 6.4°C and 17.3°C. Furthermore, **Error! Reference source not found.** shows the behavior of a temperature difference, and the maximum value of this temperature is

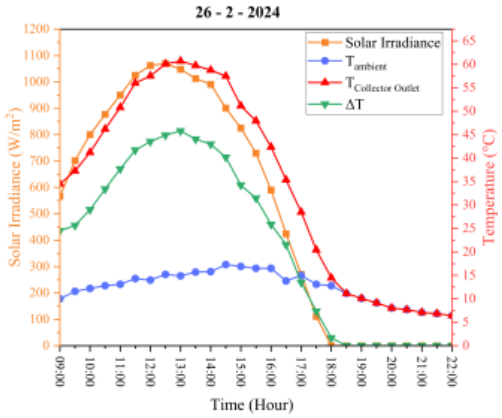

Figure 11. Variation of Solar irradiance, Collector temperature, and temperature difference with daylight time on 26 – 2 - 2024.

On March 25th, 2024, **Figure 12** show a similar behavior but different maximum and minimum values due to the ambient temperature and solar irradiation. The solar radiation intensity reaches its maximum value at the zenith, which was 1043 W/m² between 11:30 A.M. and 12:30 P.M., consequently raising the collector's outlet temperature to 63.7°C. Throughout the day, the ambient temperature varied between 11.4°C and 20.9°C. By noon, there was a temperature difference (represented as ΔT) of around 44.7°C between the solar air collector's exit temperature and the inlet ambient temperature.

Figure 13 illustrates the temperatures of air as it exits the solar air collector into the cement mortar molds storage bed, as well as the air exiting the storage bed, which are recorded over time for two different days. It is evident from **Figure 13** that inlet temperatures rise proportionally with the augmentation of solar radiation intensity throughout the duration. Additionally, the air temperature leaving the cement mortar storage bed increases gradually due to the presence of molds inside the bed, attributed to the heat absorption by the molds within the storage medium during daylight hours for thermal charging. Conversely, ambient temperature exhibits minimal variance and

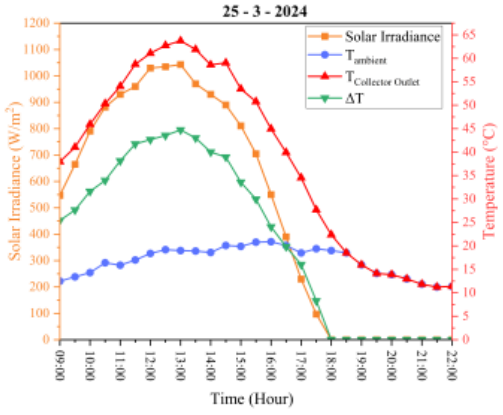

Figure 12. Variation of Solar irradiance, Collector temperature, and temperature difference with daylight time on 25 - 3 – 2024.

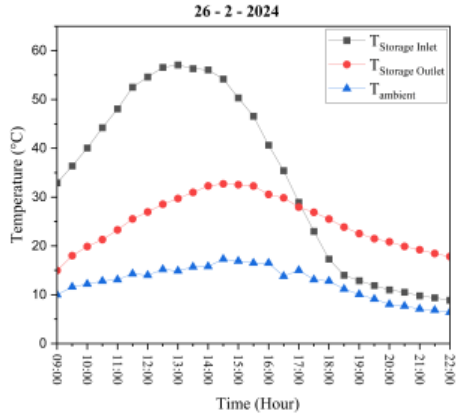

Figure 14 Variation of collector Inlet Temperature, storage inlet Temperature, and storage outlet with Time on 26 – 2 – 2024.

Figure 14 shows that the peak temperature values were recorded on March 25th, 2024, attributed to the intense solar radiation, which peaked at 1070 W/m² at 12:25 P.M., accompanied by a slight increase in ambient temperatures. After sunset, the thermal output from the cement mortar mold storage bed varied between 30 °C and 27 °C from 4:00 PM to 7:00 PM, while the ambient temperature ranged from 18 °C to 10 °C during the same period. Consequently, the discharge phase continued until 10:00 PM, at which point the temperature output from the stone storage bed was 21 °C, with the ambient temperature at 11 °C, producing a temperature differential (ΔT) of 10 °C.

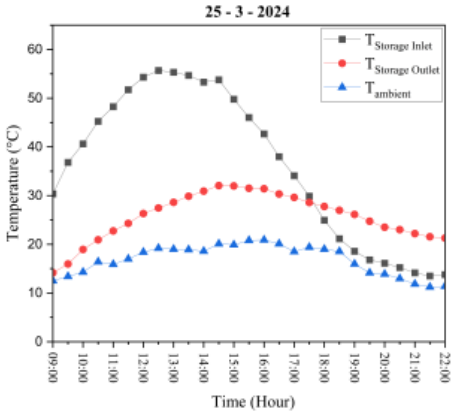

Figure 13 Variation of collector Inlet, storage inlet, and storage outlet with Time on 25 – 3 – 2024.

Figure 15 demonstrate the temperature variations across the layers of the cement mortar storage bed, which were recorded at three distinct diameters of the storage positions - bottom, middle, and top - over two separate days. The temperature of the air exiting the solar air collector enters the bottom of the cement mortar mold storage bed. The data illustrated in the **Figure 15** from the recorded temperatures by thermocouples

which are installed in the position at the bottom, middle and top of the cement mortar molds of storage bed we can show the higher temperatures of the bottom cement mortar molds have maximum values and decreasing at 17:00 until 22:00 pm. Also, the middle and Upper temperatures of the cement mortar molds decreased at 18:00 until 22:00 , clearly from the figure we can show from this figure the temperature of the middle and to of the cement mortar molds are higher than the temperature of the cement mortar molds, this

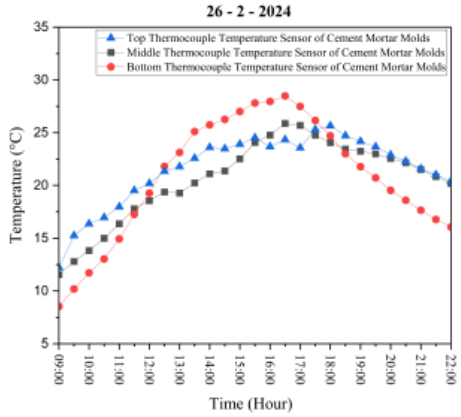

Figure 15 Variation of Upper, Middle, and Bottom Temperatures for Mortar Storage with Time on 26 – 2 – 2024.

On March 25th, 2024, **Error! Reference source not found.** show that the increased storage capacity was achieved by harnessing solar Energy from the solar air collector into the storage unit. The cement mortar molds absorbed thermal Energy, particularly between 11:00 A.M. and 16:00 P.M. during the charging process. At 4:00 P.M., during the discharge phase, the highest recorded air temperature reached 27.7 °C. Subsequently, during the 6-hour period following sunset, the stored air was released with a temperature differential (ΔT) of 10 °C until 10:00 P.M.

Figure 17 shows the difference in the amount of useful heat from the solar collector and from the storage unit over the operating hours. The useful heat from the solar collector disappears at 18:00, while the useful heat from the storage unit continues until the end of the operating period. The stored Energy continues to be recovered at an amount of about 200-230 watts until the end of the day. After sunset, we can benefit from the storage energy in the cement mortar molds, which is leads to continues the useful heat energy.

Figure 18 shows the same behavior but with a little less useful heat due to the increase in ambient temperature

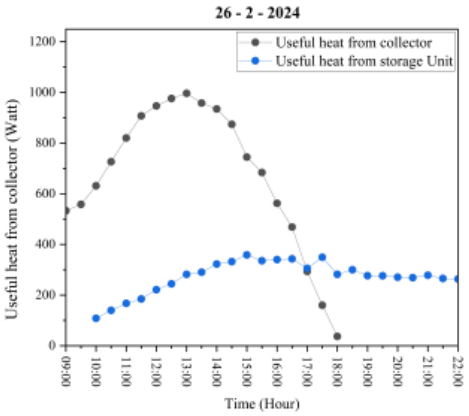

Figure 16 Variation of Useful heat with Time on 26 – 2 – 2024.

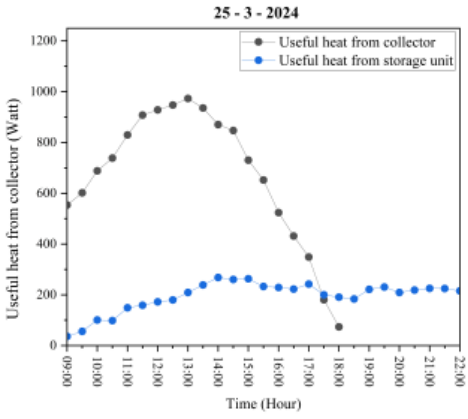

Figure 17 Variation of Useful heat with Time on 25 – 3 – 2024.

Conclusion

This research reports on the performance assessment of a latent heat thermal storage unit integrated with a flat plate-type solar air heater. During the experiment, up to 22:00 hours at night, a continuous temperature differential of 32°C to 22°C is noted at the thermal energy storage outlet. The temperature difference is noticeable. The thermal energy storage system's maximum entrance temperature is 56°C, and its highest outlet temperature was measured at 32°C throughout the day. These observations demonstrate how the system guards against overheating and ensures the output is within the necessary temperature range. The solar air dryer, used to dry fruits, vegetables, and fish, is the best device for this system. Additionally, this approach may be tailored to any specific food item. This technology has very low operating costs.

References

[1] J. Hu and G. Zhang, "Performance improvement of solar air collector based on airflow reorganization: A review," Jun. 05, 2019, *Elsevier Ltd*. doi: 10.1016/j.applthermaleng.2019.04.021.

[2] G. Murali, K. Rama Krishna Reddy, M. Trinath Sai Kumar, J. SaiManikanta, and V. Nitish Kumar Reddy, "Performance of solar aluminium can air heater using sensible heat storage," in *Materials Today: Proceedings*, Elsevier Ltd, 2020, pp. 169–174. doi: 10.1016/j.matpr.2019.04.213.

[3] S. Poppi, N. Sommerfeldt, C. Bales, H. Madani, and P. Lundqvist, "Techno-economic review of solar heat pump systems for residential heating applications," 2018, *Elsevier Ltd*. doi: 10.1016/j.rser.2017.07.041.

[4]A. E. Kabeel, A. Khalil, S. M. Shalaby, and M. E. Zayed, "Experimental investigation of thermal performance of flat and v-corrugated plate solar air heaters with and without PCM as thermal energy storage," *Energy Convers Manag*, vol. 113, pp. 264–272, Apr. 2016, doi: 10.1016/j.enconman.2016.01.068.

[5] D. L. Zhao, Y. Li, Y. J. Dai, and R. Z. Wang, "Optimal study of a solar air heating system with pebble bed energy storage," *Energy Convers Manag*, vol. 52, no. 6, pp. 2392–2400, Jun. 2011, doi: 10.1016/j.enconman.2010.12.041.

[6] O. R. Alomar, M. M. M. Salih, and H. M. Abd, "Performance analysis of single-pass solar air heater thermal collector with adding porous media and finned plate," *Energy Storage*, vol. 5, no. 5, Aug. 2023, doi: 10.1002/est2.447.

[7] V. V. Tyagi, N. L. Panwar, N. A. Rahim, and R. Kothari, "Review on solar air heating system with and without thermal energy storage system," May 2012. doi: 10.1016/j.rser.2011.12.005.

[8] H. Singh, R. P. Saini, and J. S. Saini, "A review on packed bed solar energy storage systems," Apr. 2010. doi: 10.1016/j.rser.2009.10.022.

[9] H. Zhou, Z. Lai, and K. Cen, "Experimental study on energy storage performances of packed bed with different solid materials," *Energy*, vol. 246, May 2022, doi: 10.1016/j.energy.2022.123416.

[10] A. Hassan, A. M. Nikbakht, S. Fawzia, P. K. D. V. Yarlagada, and A. Karim, "Transient analysis and techno-economic assessment of thermal energy storage integrated with solar air heater for energy management in drying," *Solar Energy*, vol. 264, Nov. 2023, doi: 10.1016/j.solener.2023.112043.

[11] A. Heydari, "Experimental analysis of hybrid dryer combined with spiral solar air heater and auxiliary heating system: Energy, exergy and economic analysis," *Renew Energy*, vol. 198, pp. 1162–1175, Oct. 2022, doi: 10.1016/j.renene.2022.08.110.

[12] C. A. Komolafe, I. O. Oluwaleye, O. Awogbemi, and C. O. Osueke, "Experimental investigation and thermal analysis of solar air heater having rectangular rib roughness on the absorber plate," *Case Studies in Thermal Engineering*, vol. 14, Sep. 2019, doi: 10.1016/j.csite.2019.100442.

[13] A. A. El-Sebaii, S. Aboul-Enein, M. R. I. Ramadan, and E. El-Bialy, "Year round performance of double pass solar air heater with packed bed," *Energy Convers Manag*, vol. 48, no. 3, pp. 990–1003, Mar. 2007, doi: 10.1016/j.enconman.2006.08.010.

[14] A. Kürklü, S. Bilgin, and O. ¨ Zkan, "A study on the solar energy storing rock-bed to heat a polyethylene tunnel type greenhouse," 2003. [Online]. Available: www.elsevier.com/locate/renene

[15] M. M. Sorour, "Performance Of A Small Sensible Heat Energy Storage Unit," 1988.

[16] D. Yogi. Goswami, *Principles of Solar Engineering*. Third Edition, 2015. doi: https://doi.org/10.1201/b18119.

Nomenclatures

M	Mass of cement mortar molds (g)
n	number of the particles
ρ_{mo}	Cement mortar molds density, (kg/m^3)
ρ_a	Air density, (kg/m^3)
V_1	total bed volume (m^3)
V_m	material volume in a packed bed (m^3)
V_{air}	air speed (m/s)
Q_c	heat energy of solar collector (W)
Q_{rc}	heat energy of recovery (W)
ṁ	mass flow rate (kg/s)
C_p	specific heat (kJ/kg °C)
T_{in}	Temperature inlet (°C)
T_{out}	Temperature outlet (°C)
I	solar radiation measured (W/m^2)
A	area (m^2)
h	surface heat-transfer coefficient (W/m^2 K)
G	superficial mass flow rate (kg/m^2. s)
K	thermal conductivity, (W/m K)

Greek Symbols

η	Efficiency (%)
μ	the viscosity (kg/m. s)
ε	Void fraction

Subscripts

SAC	Solar Air Collector
amb	Ambient
in	Inlet
out	Outlet